

Nontrivial Triplon Topology and Triplon Liquid in Kitaev-Heisenberg-type Excitonic Magnets

Pavel S. Anisimov,^{1,2} Friedemann Aust,^{1,2} Giniyat Khaliullin,³ and Maria Daghofer^{1,2}

¹*Institute for Functional Matter and Quantum Technologies,
University of Stuttgart, Pfaffenwaldring 57, 70550 Stuttgart, Germany*

²*Center for Integrated Quantum Science and Technology,
University of Stuttgart, Pfaffenwaldring 57, 70550 Stuttgart, Germany*

³*Max Planck Institute for Solid State Research, Heisenbergstraße 1, 70569 Stuttgart*

(Dated: May 1, 2019)

The combination of strong spin-orbit coupling and correlations, e.g. in ruthenates and iridates, has been proposed as a means to realize quantum materials with nontrivial topological properties. We discuss here Mott insulators where onsite spin-orbit coupling favors a local $J_{\text{tot}} = 0$ singlet ground state. We investigate excitations into a low-lying triplet, triplons, and find them to acquire nontrivial band topology in a magnetic field. We also comment on magnetic states resulting from triplon condensation, where we find, in addition to the same ordered phases known from the $J_{\text{tot}} = \frac{1}{2}$ Kitaev-Heisenberg model, a triplon liquid taking the parameter space of Kitaev's spin liquid.

Prime candidate systems for the interaction of spin-orbit coupling with substantial electronic correlations are those containing $4d$ and $5d$ transition metals, where 'topological Mott insulators' [1] or topological spin liquids were proposed. A prominent example is the prediction of Kitaev's spin liquid [2] in materials with a single hole in the t_{2g} levels [3, 4]. Strong research activity has subsequently focused on honeycomb iridates [5] and on α - RuCl_3 [6, 7]. Encouragingly, $\text{H}_3\text{LiIr}_2\text{O}_6$ does indeed not show magnetic order [8] and zig-zag order in α - RuCl_3 can be suppressed by a magnetic field [9, 10]. In the latter case, a thermal Hall effect due to the Majorana edge states has been reported [11].

Current interest has similarly been drawn to spin-orbit coupled Mott insulators with *two* holes in the t_{2g} shell. In addition to total spin $S = 1$, they would have an effective orbital angular momentum $L = 1$, and spin-orbit coupling prefers their opposite orientation into a singlet ground state $J_{\text{tot}} = 0$. On the other hand, magnetic superexchange between two ions involves the excited states with $J_{\text{tot}} > 0$. This superexchange can drive excitonic magnetism via the condensation of bosonic 'triplons' [12, 13].

While the classical limit of this scenario is governed by the same symmetries – and thus by similar magnetic ordering patterns – as the $J_{\text{tot}} = \frac{1}{2}$ scenario, the underlying degree of freedom is a superposition of the $J_{\text{tot}} = 0$ and $J_{\text{tot}} = 1$ states. In addition to opening the route to unconventional collective state like triplet superconductivity [14], this has a decisive impact on excitations, e.g. on their dispersion in the Brillouin zone. With the observation of an amplitude 'Higgs' mode, Ca_2RuO_4 has been argued to realize such a scenario close to a quantum critical point [15, 16].

Here, we investigate this scenario on the honeycomb lattice, a model that should be appropriate to compounds like Li_2RuO_3 [17] and $\text{Ag}_3\text{LiRu}_2\text{O}_6$ [18], and whose low coordination number has been proposed to make it susceptible to states with enhanced quantum

fluctuations [12]. We focus first on the regime with dominant $J_{\text{tot}} = 0$ character, i.e., where onsite spin-orbit coupling dominates over intersite superexchange, as found for d^4 iridates with a double-perovskite lattice [19–21]. We find that excitations become topologically nontrivial in magnetic fields. This implies features like protected edge states crossing triplon-band gaps, similar to the topological magnon edge states discussed as spin conductors with reduced dissipation [22, 23], and the thermal Hall effect [24–28].

We also present a phase diagram of the magnetic states emerging once the $J_{\text{tot}} = 1$ states become more dominant. We find magnetically ordered phases analogous to those of the $J_{\text{tot}} = \frac{1}{2}$ Kitaev-Heisenberg model, and also a disordered phase taking the place of Kitaev's spin liquid. This 'triplon liquid' realizes a quantum-mechanical order-by-disorder scenario, where quantum fluctuations select a unique gapped ground state from classically degenerate dimer coverings.

Model. Based on Ref. [12], we model the strongly spin-orbit coupled d^4 Mott insulators as

$$\begin{aligned}
 H = & \lambda \sum_{i,\alpha} n_{i,\alpha} + J \sum_{\langle i,j \rangle} (\mathbf{T}_i^\dagger \mathbf{T}_j - c_J \mathbf{T}_i^\dagger \mathbf{T}_j^\dagger + \text{H. c.}) \quad (1) \\
 & + K \sum_{\alpha} \sum_{\langle i,j \rangle \parallel \alpha} (T_{i,\alpha}^\dagger T_{j,\alpha} - c_K T_{i,\alpha}^\dagger T_{j,\alpha}^\dagger + \text{H. c.}) \\
 & + \Gamma \sum_{\substack{\alpha \neq \beta \neq \gamma \\ \alpha \neq \gamma}} \sum_{\langle i,j \rangle \parallel \alpha} (T_{i,\beta}^\dagger T_{j,\gamma} - c_\Gamma T_{i,\beta}^\dagger T_{j,\gamma}^\dagger + \text{H. c.}),
 \end{aligned}$$

where $T_{i,\alpha}^\dagger$ ($T_{i,\alpha}$) creates (annihilates) a triplon, i.e. a hard-core boson, with flavor $\alpha = x, y, z$ at site i . These operators are collected into vectors $\mathbf{T}_i = (T_{i,x}, T_{i,y}, T_{i,z})$. The honeycomb lattice is built of three bond directions, here likewise labeled by $\alpha = x, y, z$ so that the triplon with coupling K on a given bond bears the same index as the bond. Energy λ associated with creating a triplon is given by spin-orbit coupling separating the $J_{\text{tot}} = 0$ from the $J_{\text{tot}} = 1$ states. Couplings J , K , and Γ can be

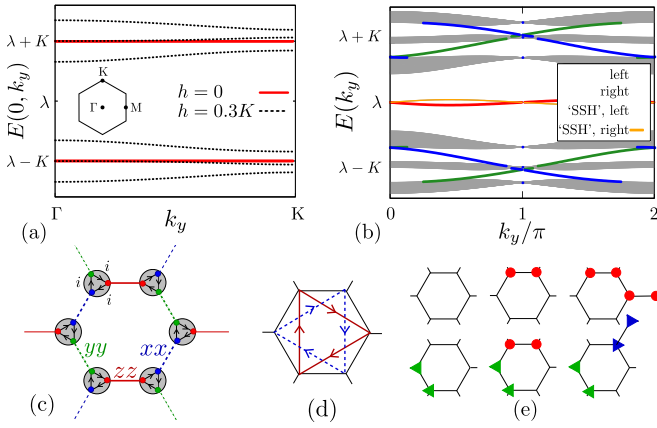


FIG. 1. (a) Triplon bands for momentum \mathbf{k} along the line $\Gamma = (0, 0)$ to $K = (0, \frac{2\pi}{\sqrt{3}})$ for dominant 'Kitaev' coupling, i.e. for $J = \Gamma = 0$, and deep within the $J_{\text{tot}} = 0$ regime, i.e. for $\lambda \gg K$. Bands are three-fold degenerate in the absence of a magnetic field and split for $\mathbf{h} = h(1, 1, 1)$ with $h = 0.3K$. Inset indicates the first Brillouin zone with three high-symmetry points. (b) Topologically nontrivial bands, with Chern numbers $C = -1, 0, 1$ from the bottom to the top, and edge states along zig-zag edges, obtained for a cylinder. (c) Decorated honeycomb lattice realized for $J, \Gamma \approx 0$ in a magnetic field \mathbf{h} perpendicular to the plane. Thick colored lines are the bonds of the honeycomb lattice, triplons are confined to a bond for $\mathbf{h} = 0$. Each shaded circle corresponds to one real-space site, $\mathbf{h} \neq 0$ allows onsite flavor transitions illustrated via triangles. (d) Next-nearest-neighbor (NNN) Dzyaloshinskii-Moriya (DM) interactions (3), D is positive (negative) for triplon hopping in the direction (opposite to) the arrows. (e) Examples for triplon configurations found in the triplon liquid; right- and left-facing triangles and circles stand for x -, y -, and z -type triplons.

estimated from second-order perturbation theory. The constants c_J , c_K , and c_Γ giving the relative strength of triplon hopping to pair creation terms depend on the microscopic processes involved. However, they are of order 1, and since we have verified that the results presented here do not depend on their precise values, we set here $c_J = c_K = c_\Gamma = 1$. The full model also features three- and four-triplon terms, but as these only become relevant once the groundstate contains an appreciable number of triplons, their influence on triplon excitations of the $J_{\text{tot}} = 0$ state and on its ordering tendencies (before order sets it) are small. They are neglected here, but are shortly discussed in the supplemental material [29].

For 90° bond angles, dominant oxygen-mediated electron hopping t and neglecting Hund's rule, K becomes $\approx -J$ so that every triplon flavor can move on two kinds of bonds along a zig-zag line through the honeycomb lattice [12]. Hopping t' due to direct overlap between the d orbitals leads to $K \gg J > 0$; and if both t and t' are present, $\Gamma \propto tt'$ becomes active. Further, Hund's rule coupling promotes FM exchange [13], processes via e_g orbitals might also contribute [4, 30], and a honeycomb lat-

tice can also arise with 180° bond angles in 'dice-lattice' bilayer heterostructures [31]. Since a large variety of parameter combinations are possible, we treat J , K and Γ as material-dependent and vary them in the present study.

Nontrivial triplon topology. For $\lambda \gg J, K, \Gamma$, the $J_{\text{tot}} = 0$ state determines the ground state, but once a triplon is excited, it can move to another site via the $T_i^\dagger T_j$ terms of (1). The $T_i^\dagger T_j^\dagger$ terms enter in order $\frac{1}{\lambda}$, and we consequently neglect them in this analysis of excitations deep within the $J_{\text{tot}} = 0$ phase, see also Ref. 24.

The bands described by (1) have Chern number $C = 0$, but can nevertheless show edge states. These can be most easily seen for the extreme "Kitaev" limit $\lambda \gg |K| > 0$ and $J = \Gamma = 0$, where one finds two groups of threefold degenerate dispersionless bands at energies $\lambda \pm K$, see Fig. 1(a). Each corresponds to one triplon flavor and eigenstates are perfectly localized on isolated bonds of the honeycomb lattice, see Fig. 1(c). If a zig-zag edge cuts all z bonds along a vertical line, z -triplon states on the edge sites have no site to hop to, so that their energy becomes λ instead of $\lambda \pm K$, see Fig. 1(b). Such states can be ascribed a topological origin [32] that is related to the Zak phase [33] and to the topological end states of a Su-Shrieffer-Heeger (SSH) chain [34]. Very recently, a model supporting such states has been argued to describe neutron-scattering data for $\text{Ba}_2\text{CuSi}_2\text{O}_6\text{Cl}_2$ [34].

The 'SSH' edge states discussed above do not cross the gap between triplon bands, are localized to isolated sites for $|K| \gg |J|, |\Gamma|$, and would thus not be good candidates for transport. Edge states between bands with different Chern numbers, which do cross gaps and support a thermal Hall effect, need broken time-reversal symmetry. One possibility is a magnetic field $H_m = \mathbf{h} \sum_i \mathbf{M}_i$, which couples to the magnetic moment on site i ,

$$\mathbf{M}_i = -i\sqrt{6}(\mathbf{T}_i - \mathbf{T}_i^\dagger) + ig\mathbf{T}_i^\dagger \times \mathbf{T}_i, \quad (2)$$

with $g = \frac{1}{2}$ [12]. Again, the first term linear in triplon operators is suppressed at large λ .

The second term in (2), which drives onsite flavor transitions, can as before be discussed most clearly for the extreme "Kitaev" limit $\lambda \gg |K| > 0$ and $J = \Gamma = 0$. Starting from the degenerate dispersionless bands of Fig. 1(a), a field $\mathbf{h} \parallel (1, 1, 1)$ [i.e. perpendicular to the honeycomb plane] allows transitions between flavors on each site. Triplons are then no longer localized to a single bond and bands become dispersive, see Fig. 1(a) and (b). As illustrated in the cartoon Fig. 1(c), the system in fact becomes equivalent to a decorated honeycomb lattice, where topologically nontrivial bands can arise [35]. As a result of the imaginary phase i , see Eq. (2) and Fig. 1(c), the top and bottom band of each triplet acquires a nontrivial Chern number $C = \pm 1$, and the two bands are connected by protected edge states, see Fig. 1(b).

Figure 2 gives a phase diagram in J - K parameter space, with topologically nontrivial bands almost every-

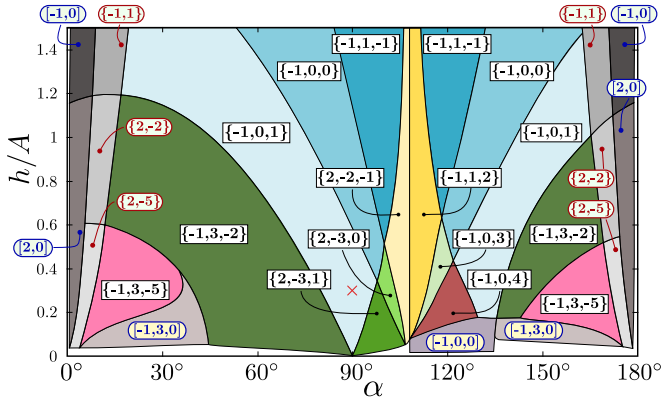


FIG. 2. ‘Phase diagram’ of the topologically nontrivial triplon excitations as a function of the magnetic field $\mathbf{h} = h(1, 1, 1)$ and angle α defined as $J = A \cos \alpha$, $K = A \sin \alpha$. We set $\Gamma = 0$ and consider the $J_{\text{tot}} = 0$ regime, where $\lambda \gg A$ drops out of the calculation [24]. For parameter values crudely estimated to apply to transition-metal d^4 systems [12], $h = 0.1A$ corresponds to ≈ 1 Tesla. The numbers given for each phase are Chern numbers: curly brackets refer to phases with an even number of triplon bands (four or six), where SSH-type edge states may additionally occur in the gap around λ . The Chern numbers are for the lower two or three bands, those of the upper two or three are opposite. Square brackets refer to phases where the middle gap has closed so that there is an odd number of bands and no SSH-type edge states. Since our spectra are always symmetric, the middle band has to have Chern number 0, the first one or two indices give the Chern number(s) of the band(s) below the middle band. The cross at $\alpha = 90^\circ$ and $h = 0.3A$ indicates parameter values used in Fig. 1(a,b).

where. Gaps between Chern bands can be quite small and energy ranges of bands may in fact overlap with indirect gaps; more robust gaps are generally found for intermediate α (i.e. for large K). Allowing $\Gamma \neq 0$ significantly affects phase boundaries (not shown), but topological band character persists. In general, finite magnetic fields are needed, but correspond to achievable strengths of a few Tesla for estimated parameters [12]. This implies that t_{2g}^4 honeycomb insulators provide a viable route to the observation of triplon bands with Chern numbers as high as $C = 5$.

Nontrivial triplon topology in coupled intersite-dimer systems arises through DM interactions [24, 25, 32, 36], which are symmetry-allowed on NNN-bonds and take the form:

$$H_{\text{DM}} = \sum_{\langle\langle i,j \rangle\rangle} \mathbf{D}_{ij} \cdot \mathbf{T}_i^\dagger \times \mathbf{T}_j, \quad (3)$$

with $\mathbf{D}_{ij} = \pm D(1, 1, 1)$, i.e. perpendicular to the plane; $\langle\langle i,j \rangle\rangle$ denotes NNNs and the + (−) sign applies to (anti-) clockwise motion within a hexagon, see Fig. 1(d). The similarity of DM term (3) and magnetization (2) is obvious. We have found DM interactions to support Chern numbers $C = \pm 1$ in the absence of a magnetic field, e.g.

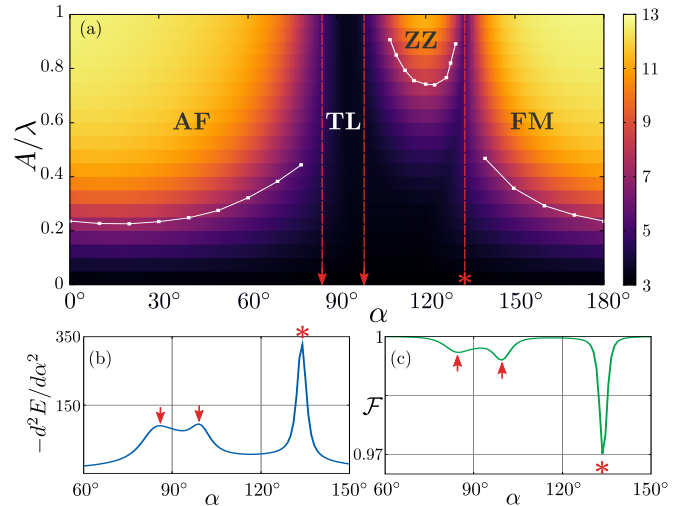


FIG. 3. Magnetic phase diagram. (a) Phase diagram based on the spin-structure factor $S^{\alpha,\beta}(\mathbf{k})$, see (4), obtained by ED of a 12-site cluster. Couplings are parameterized as $J = A \cos \alpha$, $K = A \sin \alpha$, $\Gamma = 0$. Color refers to the maximal $S^{\alpha,\beta}(\mathbf{k})$; (AF), FM, and ZZ indicate (anti)ferromagnetic and zigzag order. White dots give the inflection point of $S^{\alpha,\beta}(\mathbf{k})$ vs. A . TL labels the region with appreciable triplon density ($\rightarrow 0.333$ for large A) but small $S^{\alpha,\beta}(\mathbf{k})$, i.e., the ‘triplon liquid’. (b) Fidelity $\langle \phi_0(\alpha) | \phi_0(\alpha + d\alpha) \rangle$ and (c) second derivative of the ground-state energy for $A = \lambda$. Arrows and asterisk indicate the positions of the peaks in (b) and (c).

for $J = 1$, $\Gamma = K = 0$, and $\mathbf{h} = 0$. However, the gaps are here rather fragile and nontrivial band topology is lost for finite K and Γ of the order of D . As NNN DM terms are in general expected to be rather smaller than NN interactions K and Γ , this suggests a minor role for the former [37].

Magnetic Phase Diagram and triplon liquid. While a detailed investigation of the model’s magnetic phases is beyond the scope of this work [38], we shortly discuss their basic features. The ordering vector expected for a magnetically ordered phase is the one where the triplon excitations first reach zero energy. The $T_i^\dagger T_j^\dagger$ terms in the Hamiltonian have to be included here. We have accordingly used a Bogoliubov-de Gennes transformation [39], which neglects the hard-core constraint of the triplons, and exact diagonalization (ED), which is restricted to small clusters. We additionally interpolated between these two approaches using cluster-perturbation theory, which incorporates the hard-core constraint within the directly solved cluster.

For $\Gamma = 0$, the phase diagram obtained from ED is given in Fig. 3(a). The dark region in the middle corresponds to the $J_{\text{tot}} = 0$ regime, where hardly any triplons are mixed into the ground state $|\phi_0\rangle$ and where magnetic structure factors

$$S^{\alpha,\beta}(\mathbf{k}) = \left\| \sum_i e^{i\mathbf{k}\cdot\mathbf{r}_i} (T_{i,\alpha}^\dagger - T_{i,\beta}) |\phi_0\rangle \right\|^2 \quad (4)$$

are thus small for any \mathbf{k} . The ground-state fidelity in Fig. 3(b) as well as the second derivative of the ground-state energy in Fig. 3(c) have here a single peak, which indicates a first-order phase transition. The canonical-boson treatment and cluster-perturbation theory agree with these phase boundaries, which furthermore correspond more closely to classical predictions than in the $J_{\text{tot}} = \frac{1}{2}$ Kitaev-Heisenberg model [40]. As in a classical model, our phase diagram going from 0 to 180° (i.e. for $K > 0$) perfectly repeats itself for the negative- K part going from 180° to 360° (except that FM and AF change places and that zigzag becomes stripy).

Differences between the classical analysis and ED arise near the 'Kitaev' limits $J = \Gamma = 0$. The fidelity and second energy derivative obtained from ED, see Figs. 3(b,c), argue here against the single first-order transition of the classical scenario and in favor of an intermediate phase in a narrow but finite parameter regime around the Kitaev points. With a triplon density $n \approx 0.33$ at large K (somewhat below the $n \approx 0.45$ of the ordered phases), the phase clearly differs from the vacuum with $n \approx 0$, and we term it a 'triplon liquid'. We have found the phase to be stable against small $\Gamma \neq 0$, its stability range is similar to that of Kitaev's spin liquid in the corresponding $J_{\text{tot}} = \frac{1}{2}$ model [41]. The character of the present triplon liquid, however, differs from Kitaev's spin liquid, as we find here no topological degeneracy.

For $J = \Gamma = 0$, the ground state contains, in addition to the vacuum state, only configurations where x - (y -, z -) bosons sit on both ends of x - (y -, z -) bonds, see Fig. 1(e) for examples. This observation allows us to restrict the Hilbert space to such dimer configurations and to obtain ground states of clusters with up to 30 sites; excitations going beyond this restricted Hilbert space can be obtained for up to 18 sites. Based on the dimer observation, one can moreover see that any structure factors (4) are strictly short range, and we find numerically no indications for bond order either.

Semi-classically, we expect for $J = \Gamma = 0$ an infinitely degenerate ground-state manifold of dimer coverings, with each dimer in a superposition of 'empty' and 'occupied' and an energy of $E_c = -K/2$ per site for $K \gg \lambda$. The triplon liquid has a non-degenerate ground state with markedly lower energy. This quantum-mechanical order-by-disorder mechanism is largely mediated by the vacuum state, which is shared between the dimer coverings and makes them non-orthogonal.

The energy gap between the ground state and the rest of the spectrum allows the triplon liquid to survive small $J, \Gamma \neq 0$. We have also assessed the impact of three- and four-triplon terms that were left out of the Hamiltonian (1), but are present at sizeable triplon densities [12]. We have found them to leave the scenario of Fig. 3 intact, i.e., the triplon liquid without long-range order remains as an intermediate phase between the zig-zag and Néel AF phases [29].

Conclusions. We analyzed a singlet-triplet model for honeycomb compounds with a strongly correlated and spin-orbit coupled t_{2g}^4 configuration, as e.g. appropriate for materials like $\text{Ag}_3\text{LiRu}_2\text{O}_6$ [18] and Li_2RuO_3 [17]. The latter might in fact be close to a quantum critical point, because its magnetic state differs between powder [42] and single-crystal samples [43]. This would be consistent with a close competition that is decided by the triplons's coupling to the lattice. For strong intersite superexchange, we find magnetically ordered states (Néel, stripe and zig-zag AF and FM) as well as a triplon liquid stabilized out of classically degenerate dimer coverings via a quantum order-by-disorder mechanism.

At weaker superexchange, where the ground state is dominated by the $J_{\text{tot}} = 0$ state of the ion, excitations are found to be topologically nontrivial as soon as orbital anisotropies become relevant. Topologically nontrivial triplon bands have been proposed [24] and found to agree with neutron scattering data [44] for $\text{SrCu}_2(\text{BO}_3)_2$, whose ground state consists of singlets on dimers; the discussion has since been extended to other geometries [25, 32, 36]. Topological triplon states in these dimer systems rely on DM interactions, which we found to compete with symmetric anisotropic exchange in the present *onsite*-singlet systems. Consequently, magnetic fields perpendicular to the plane appear a more promising route towards nontrivial triplon topology when anisotropic couplings can be expected to dominate over DM interactions.

In addition to the $J_{\text{tot}} = 0$ regime discussed above, topologically nontrivial excitations are expected to persist into the FM phase, analogous to the nontrivial magnon topology in ferromagnetically polarized states of the $J_{\text{tot}} = \frac{1}{2}$ Kitaev model [45, 46]. The AF patterns require a more detailed symmetry analysis [47], but may also harbor nontrivial magnon bands. Finally, potential topological properties of the triplon liquid present an intriguing question once a magnetic field renders the underlying single-triplon states nontrivial.

We thank G. Jackeli and J. Chaloupka for many fruitful discussions. This research was supported by the Deutsche Forschungsgemeinschaft, via the Emmy-Noether program (DA 1235/1-1) and FOR1807 (DA 1235/5-1).

-
- [1] D. Pesin and L. Balents, Nat. Phys. **6**, 376 (2010).
 - [2] A. Kitaev, Annals of Physics **321**, 2 (2006).
 - [3] G. Jackeli and G. Khaliullin, Phys. Rev. Lett. **102**, 017205 (2009).
 - [4] J. Chaloupka, G. Jackeli, and G. Khaliullin, Phys. Rev. Lett. **110**, 097204 (2013).
 - [5] S. M. Winter, A. A. Tsirlin, M. Daghofer, J. van den Brink, Y. Singh, P. Gegenwart, and R. Valentí, J. Phys. Condens. Matter **29**, 493002 (2017).

- [6] K. W. Plumb, J. P. Clancy, L. J. Sandilands, V. V. Shankar, Y. F. Hu, K. S. Burch, H.-Y. Kee, and Y.-J. Kim, *Phys. Rev. B* **90**, 041112 (2014).
- [7] Y. Kubota, H. Tanaka, T. Ono, Y. Narumi, and K. Kindo, *Phys. Rev. B* **91**, 094422 (2015).
- [8] K. Kitagawa, T. Takayama, Y. Matsumoto, A. Kato, R. Takano, Y. Kishimoto, S. Bette, R. Dinnebier, G. Jackeli, and H. Takagi, *Nature* **554**, 341 (2018).
- [9] R. Yadav, N. A. Bogdanov, V. M. Katukuri, S. Nishimoto, J. van den Brink, and L. Hozoi, *Sci. Rep.* **6**, 37925 (2016).
- [10] S.-H. Baek, S.-H. Do, K.-Y. Choi, Y. S. Kwon, A. U. B. Wolter, S. Nishimoto, J. van den Brink, and B. Büchner, *Phys. Rev. Lett.* **119**, 037201 (2017).
- [11] Y. Kasahara, T. Ohnishi, Y. Mizukami, O. Tanaka, S. Ma, K. Sugii, N. Kurita, H. Tanaka, J. Nasu, Y. Motome, T. Shibauchi, and Y. Matsuda, *Nature* **559**, 227 (2018).
- [12] G. Khaliullin, *Phys. Rev. Lett.* **111**, 197201 (2013).
- [13] O. N. Meetei, W. S. Cole, M. Randeria, and N. Trivedi, *Phys. Rev. B* **91**, 054412 (2015).
- [14] J. Chaloupka and G. Khaliullin, *Phys. Rev. Lett.* **116**, 017203 (2016).
- [15] A. Jain, M. Krautloher, J. Porras, G. Ryu, D. Chen, D. Abernathy, J. Park, A. Ivanov, J. Chaloupka, G. Khaliullin, B. Keimer, and B. Kim, *Nat. Phys.* **13**, 633 (2017).
- [16] S.-M. Souliou, J. Chaloupka, G. Khaliullin, G. Ryu, A. Jain, B. J. Kim, M. Le Tacon, and B. Keimer, *Phys. Rev. Lett.* **119**, 067201 (2017).
- [17] Y. Miura, Y. Yasui, M. Sato, N. Igawa, and K. Kakurai, *J. Phys. Soc. Jpn.* **76**, 033705 (2007).
- [18] S. A. J. Kimber, C. D. Ling, D. J. P. Morris, A. Chemseddine, P. F. Henry, and D. N. Argyriou, *J. Mater. Chem.* **20**, 8021 (2010).
- [19] K. Pajskr, P. Novák, V. Pokorný, J. Kolorenč, R. Arita, and J. Kuneš, *Phys. Rev. B* **93**, 035129 (2016).
- [20] S. Fuchs, T. Dey, G. Aslan-Cansever, A. Maljuk, S. Wurmehl, B. Büchner, and V. Kataev, *Phys. Rev. Lett.* **120**, 237204 (2018).
- [21] A. J. Kim, H. O. Jeschke, P. Werner, and R. Valentí, *Phys. Rev. Lett.* **118**, 086401 (2017).
- [22] R. Shindou, R. Matsumoto, S. Murakami, and J.-i. Ohe, *Phys. Rev. B* **87**, 174427 (2013).
- [23] A. Mook, J. Henk, and I. Mertig, *Phys. Rev. B* **91**, 174409 (2015).
- [24] J. Romhányi, K. Penc, and R. Ganesh, *Nat. Commun.* **6**, 6805 (2015).
- [25] M. Malki and K. P. Schmidt, *Phys. Rev. B* **95**, 195137 (2017).
- [26] A. Mook, J. Henk, and I. Mertig, *Phys. Rev. B* **89**, 134409 (2014).
- [27] S. Murakami and A. Okamoto, *J. Phys. Soc. Jpn.* **86**, 011010 (2017).
- [28] Y. Onose, T. Ideue, H. Katsura, Y. Shiomi, N. Nagaosa, and Y. Tokura, *Science* **329**, 297 (2010).
- [29] See Supplemental Material at ... for the three- and four-boson terms and their impact on our results.
- [30] G. Khaliullin, *Prog. Theor. Phys. Suppl.* **160**, 155 (2005).
- [31] S. Okamoto, *Phys. Rev. Lett.* **110**, 066403 (2013).
- [32] D. G. Joshi and A. P. Schnyder, (2018), arXiv:1809.06387.
- [33] G. van Miert, C. Ortix, and C. M. Smith, *2D Materials* **4**, 015023 (2017).
- [34] K. Nawa, K. Tanaka, N. Kurita, T. J. Sato, H. Sugiyama, H. Uekusa, S. Ohira-Kawamura, K. Nakajima, and H. Tanaka, (2018), arXiv:1810.08931.
- [35] A. Rüegg, J. Wen, and G. A. Fiete, *Phys. Rev. B* **81**, 205115 (2010).
- [36] D. G. Joshi and A. P. Schnyder, *Phys. Rev. B* **96**, 220405 (2017).
- [37] DM interactions can gain in importance if a trigonal crystal field $\Delta \sum_{\alpha \neq \beta} T_{\alpha}^{\dagger} T_{\beta}$ splits the a_{1g} triplon mode off the e'_{g} modes. Anisotropies due to K and Γ then average out, and the DM interaction together with J yields a perfect analogy to Haldane's anomalous quantum-Hall-effect model [48] with Chern numbers ± 1 .
- [38] An extensive ED study will be presented elsewhere, J. Chaloupka and G. Khaliullin, to be published.
- [39] S. Gopalan, T. M. Rice, and M. Sigrist, *Phys. Rev. B* **49**, 8901 (1994).
- [40] D. Gotfryd, J. Rusnačko, K. Wohlfeld, G. Jackeli, J. Chaloupka, and A. M. Oleś, *Phys. Rev. B* **95**, 024426 (2017).
- [41] J. G. Rau, E. K.-H. Lee, and H.-Y. Kee, *Phys. Rev. Lett.* **112**, 077204 (2014).
- [42] J. Park, T.-Y. Tan, D. T. Adroja, A. Daoud-Aladine, S. Choi, D.-Y. Cho, S.-H. Lee, J. Kim, H. Sim, T. Morioka, H. Nojiri, V. V. Krishnamurthy, P. Manuel, M. R. Lees, S. V. Streltsov, D. I. Khomskii, and J.-G. Park, *Sci. Rep.* **6**, 25238 (2016).
- [43] J. C. Wang, J. Terzic, T. F. Qi, F. Ye, S. J. Yuan, S. Aswartham, S. V. Streltsov, D. I. Khomskii, R. K. Kaul, and G. Cao, *Phys. Rev. B* **90**, 161110 (2014).
- [44] P. A. McClarty, F. Krüger, T. Guidi, S. F. Parker, K. Refson, A. W. Parker, D. Prabhakaran, and R. Coldea, *Nat. Phys.* **13**, 736 (2017).
- [45] D. G. Joshi, *Phys. Rev. B* **98**, 060405 (2018).
- [46] P. A. McClarty, X.-Y. Dong, M. Gohlke, J. G. Rau, F. Pollmann, R. Moessner, and K. Penc, *Phys. Rev. B* **98**, 060404 (2018).
- [47] F. Lu and Y.-M. Lu, (2018), arXiv:1807.05232.
- [48] F. D. M. Haldane, *Phys. Rev. Lett.* **61**, 2015 (1988).

Supplemental Materials: Nontrivial Triplon Topology and Triplon Liquid in Kitaev-Heisenberg-type Excitonic Magnets

We present the three- and four-triplon terms of the Hamiltonian and verify that the triplon liquid remains stable when they are included.

The effective Hamiltonian in terms of singlet and triplet states, obtained in second-order perturbation theory, can be written as

$$H = \lambda \sum_{i,\alpha} n_{i,\alpha} + \sum_{\alpha} \sum_{\langle i,j \rangle \| \alpha} (h_2^\alpha + h_3^\alpha + h_4^\alpha)_{ij}. \quad (\text{S1})$$

The first term is spin-orbit coupling favoring the onsite singlet, while the sum over the nearest neighbors $\langle i, j \rangle$ parallel to the three directions $\alpha = x, y, z$ contains terms with two, three, or four triplon operators $T_{i,\alpha}^\dagger$ or $T_{i,\alpha}$.

When taking direct d - d hopping t' into account in addition to oxygen-mediated t used in Ref. S1, but still neglecting Hund's-rule coupling and crystal fields, the bilinear contribution along a bond in z direction becomes

$$\begin{aligned} h_2^z = & \left(\frac{2t^2}{3U} + \frac{1t'^2}{6U} \right) (T_{i,x}^\dagger T_{j,x} + T_{i,y}^\dagger T_{j,y} + \text{H. c.}) \\ & - \left(\frac{5t^2}{6U} + \frac{1t'^2}{6U} \right) (T_{i,x}^\dagger T_{j,x}^\dagger + T_{i,y}^\dagger T_{j,y}^\dagger + \text{H. c.}) \\ & + \frac{2t'^2}{3U} (T_{i,z}^\dagger T_{j,z} - T_{i,z} T_{j,z}^\dagger + \text{H. c.}) \\ & + \frac{tt'}{U} \left(\frac{1}{6} T_{i,x}^\dagger T_{j,y} - \frac{1}{3} T_{i,x}^\dagger T_{j,y}^\dagger + \text{H. c.} \right). \quad (\text{S2}) \end{aligned}$$

Couplings on the other bonds are obtained by cyclic permutation.

While this Hamiltonian yields the form and symmetry of superexchange terms, it neglects many processes alluded to in the main text, especially Hund's-rule coupling and any orbitals beyond the t_{2g} manifold. As has been frequently done in the analogous $J_{\text{tot}} = \frac{1}{2}$ model, we thus allow the couplings to vary rather freely. In the main text, which discusses only the bilinear terms (S2), this is done by assigning constants J , K , and Γ to isotropic, directional and flavor changing terms, respectively. While their dependence on t , t' , and U can be calculated from second-order perturbation theory, they are instead used as free parameters to take into account any neglected processes.

This approach of choosing J , K , and Γ connects easily to the literature on the $J_{\text{tot}} = \frac{1}{2}$ model, but it is not clear how to generalize it to the couplings arising the three- and four-boson terms introduced below. We thus instead introduce parameters $X = \frac{t^2}{U}$, $Y = \frac{t'^2}{U}$, and $Z = \frac{tt'}{U}$ that determine two- as well as three- and four-triplon contributions. In order to allow for processes not included in second-order perturbation theory, X , Y , and Z are then varied independently of each other and are also allowed to become negative.

The three- and four-boson terms can mostly be neglected when addressing the symmetry-breaking phase transitions into the ordered states, because triplon densities are expected to be small around a second-order symmetry-breaking transition. However, they could affect the triplon liquid, where they might stabilize magnetic order once triplon densities are substantial. We thus check their impact on the phases around the Kitaev point. Since $\Gamma \propto Z$ is not essential for this issue, we set in the following $Z = 0$ and leave the corresponding terms out for simplicity.

The three-triplon terms, except the terms $\propto Z \propto tt'$ that are left out here, are

$$\begin{aligned} h_3^z = & \frac{1}{\sqrt{24}} \frac{t^2 + t'^2}{U} (T_{i,x} T_{j,y}^\dagger T_{j,z} - T_{i,y} T_{j,x}^\dagger T_{j,z}) \\ & + \left(\frac{1}{\sqrt{6}} \frac{t^2}{U} + \frac{1}{\sqrt{24}} \frac{t'^2}{U} \right) (T_{i,y} T_{j,z}^\dagger T_{j,x} - T_{i,x} T_{j,z}^\dagger T_{j,y}) \\ & + \sqrt{\frac{3}{8}} \frac{t^2}{U} (T_{i,z} T_{j,x}^\dagger T_{j,y} - T_{i,z} T_{j,y}^\dagger T_{j,x}) + \text{H. c.} + i \leftrightarrow j, \quad (\text{S3}) \end{aligned}$$

and cyclic permutations, the terms $\propto t^2$ can also be found in Ref. S1. The four-triplon-terms can conveniently be split into diagonal and off-diagonal parts $h_4 \equiv h_{4,\text{diag}} + h_{4,\text{off}}$. The diagonal part

$$\begin{aligned} h_{4,\text{diag}}^z = & \frac{t^2}{U} \left[2(n_i^s n_j^s + n_i^s n_j^z + n_i^z n_j^s + \mathbf{n}_i \cdot \mathbf{n}_j) \right. \\ & + \frac{9}{4} (n_i^x n_j^y + n_i^y n_j^x + n_i^x n_j^z + n_i^z n_j^x + n_i^y n_j^z + n_i^z n_j^y) \\ & \left. + \frac{13}{6} (n_i^s n_j^x + n_i^s n_j^y + n_i^x n_j^s + n_i^y n_j^s) \right] \\ & + \frac{t'^2}{U} \left[\frac{16}{9} n_i^s n_j^s + 3n_i^z n_j^z + \frac{7}{3} (n_i^s n_j^z + n_i^z n_j^s) \right. \\ & + \frac{3}{2} (n_i^s n_j^x + n_i^s n_j^y + n_i^x n_j^s + n_i^y n_j^s) \\ & + \frac{5}{4} (n_i^x n_j^x + n_i^y n_j^y + n_i^x n_j^y + n_i^y n_j^x) \\ & \left. + 2(n_i^x n_j^z + n_i^y n_j^z + n_i^z n_j^x + n_i^z n_j^y) \right], \quad (\text{S4}) \end{aligned}$$

is written in terms of triplon-number operators $n_j^\alpha = T_{j,\alpha}^\dagger T_{j,\alpha}$ as well as singlet-number operator $n_j^s = 1 - \sum_\alpha n_j^\alpha$.

The off-diagonal part is

$$\begin{aligned}
h_{4,\text{off}}^z = & -\frac{1}{4} \frac{t^2 + t'^2}{U} (T_{i,x}^\dagger T_{i,z} T_{j,x}^\dagger T_{j,z} + T_{i,y}^\dagger T_{i,z} T_{j,y}^\dagger T_{j,z}) \\
& -\frac{1}{4} \frac{t^2}{U} T_{i,x}^\dagger T_{i,y} T_{j,x}^\dagger T_{j,y} \\
& +\frac{1}{4} \frac{t'^2}{U} (T_{i,x}^\dagger T_{i,z} T_{j,z}^\dagger T_{j,x} + T_{i,y}^\dagger T_{i,z} T_{j,z}^\dagger T_{j,y}) \\
& +\frac{1}{2} \frac{t^2}{U} T_{i,x}^\dagger T_{i,y} T_{j,y}^\dagger T_{j,x} + \text{H. c.}, \quad (\text{S5})
\end{aligned}$$

and cyclic permutations.

In order to revisit the magnetic phase diagram around $\alpha = 90^\circ$ given in Fig. 3 of the main text, we have to relate new parameters $X = \frac{t^2}{U}$, and $Y = \frac{t'^2}{U}$ to J and K , resp. A and α , of the main text. We had there additionally chosen $c_K = c_J = 1$, i.e., set the couplings in front of terms like $T^\dagger T$ equal to those in front of $T^\dagger T^\dagger$. As can be seen in Eq. (S2), this holds exactly for contributions $\propto Y = \frac{t'^2}{U}$, which dominate near the Kitaev point, but not for those $\propto X = \frac{t^2}{U}$, where the precise ratio is $\frac{5}{4}$. The physical meaning of using $c_J = c_K = 1$ throughout is best seen by rewriting Eq. (S2) in terms of dipolar operators $\mathbf{v} = i(\mathbf{T}^\dagger - \mathbf{T})$ and quadrupolar operators $\mathbf{u} = \mathbf{T}^\dagger + \mathbf{T}$. Setting $c_J = c_K = 1$ then amounts to neglecting quadrupolar terms, which is often justified [S12]. Moreover, they are in fact small here, close to the Kitaev point, and do not affect our results, as we show below.

Following the above considerations, we identify J and K of the main text with the isotropic and directional couplings of the dipolar fields, i.e.,

$$J = A \sin \alpha = \frac{1}{2} \left(\frac{2}{3} X + \frac{5}{6} Y \right) + \frac{1}{6} Y = \frac{3}{4} X + \frac{1}{6} Y \quad (\text{S6})$$

$$K = A \sin \alpha = \frac{2}{3} Y - J = \frac{1}{2} Y - \frac{3}{4} X. \quad (\text{S7})$$

Coupling parameters X and Y are thus obtained from J and K (resp. A and α) and inserted into (S3) - (S5) to determine the full triplon Hamiltonian (S1).

Figure S1(a) and (b) show the fidelity and second derivative $\frac{d^2 E(\alpha)}{d\alpha^2}$ of the ground state energy depending on α and for $A = \lambda$. We see that the substantial triplon densities allow h_3 and h_4 and the quadrupolar terms, which are here all included, to affect the phase boundaries to some extent. However, the interpretation of the main text remains unchanged, i.e., we find a direct first-order transitions between FM and zig-zag phases (at $\alpha \approx 135^\circ$) but an intermediate regime separating AF and zig-zag phases around the 'Kitaev' point for $87^\circ \lesssim \alpha \lesssim 104^\circ$.

The spin-structure factor of Fig. S1(c) again shows some quantitative changes, but remains qualitatively the same. In particular, three- and four-boson terms do not stabilize magnetic order in this intermediate regime, the triplon liquid. The liquid appears to be protected by the

energy gap separating its ground state from the rest of the spectrum. Additionally, a triplon density of roughly $\frac{1}{3}$, even for $A \gg \lambda$ (not shown), implies that triplons do not too often occupy nearest-neighbor sites.

[S1] G. Khaliullin, Phys. Rev. Lett. **111**, 197201 (2013).

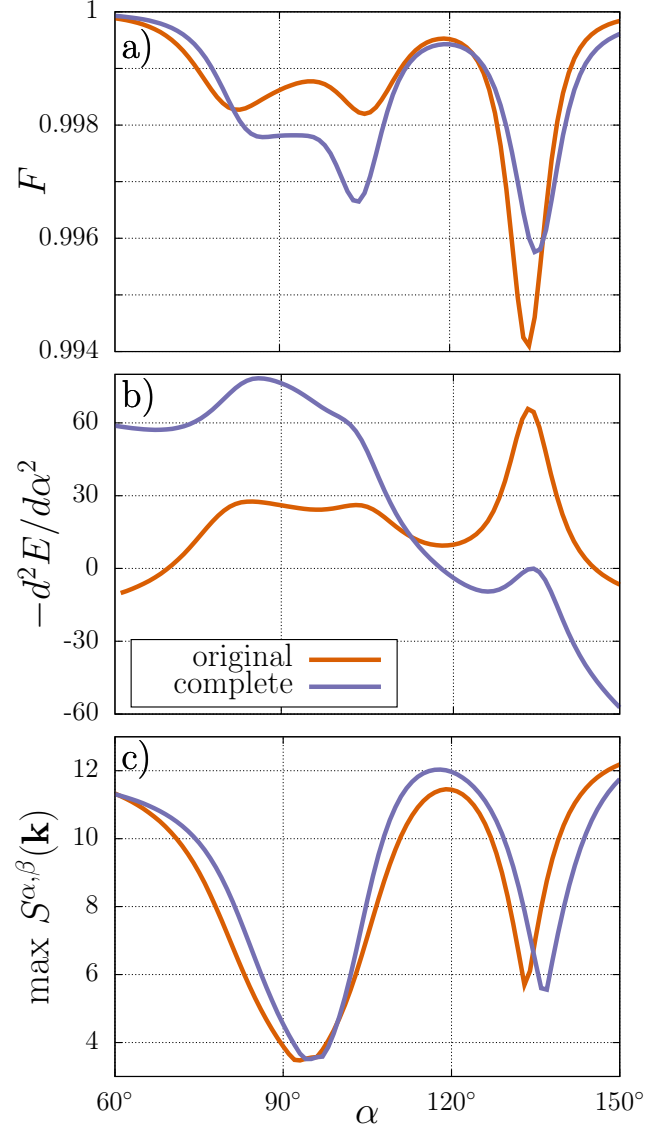


FIG. S1. Impact of three- and four-boson terms on magnetic phase transitions depending on α for $A = \lambda$. Parameters $X = \frac{t^2}{U}$ and $Y = \frac{t'^2}{U}$ of the Hamiltonian (S1) are determined from (S6) and (S7), $Z = \Gamma = 0$. (a) Shows the fidelity (b) the second energy derivative $d^2E(\alpha)/d\alpha^2$ and (c) the maximal spin-structure factor for full Hamiltonian (orange) and the Hamiltonian of the main text (purple), i.e. without h_3 and h_4 and without quadrupolar contributions.